doi:10.26443/seismica.v3i1.1190

Extensional failure in a weak slab under slab pull – the 2023 M_w 6.4 Quiché, Guatemala, earthquake

Timothy J. Craig * [1], **Amber Hull** [2]

[1]COMET, Institute for Geophysics and Tectonics, School of Earth and Environment, University of Leeds, Leeds, UK, [2]Institute for Geophysics and Tectonics, School of Earth and Environment, University of Leeds, Leeds, UK

Author contributions: *Conceptualization*: TJC. *Formal Analysis*: TJC, AH. *Investigation*: TJC, AH. *Writing - original draft*: TJC. *Writing - Review & Editing*: TJC, AH. *Supervision*: TJC. *Funding acquisition*: TJC.

Abstract The 2023 M_w 6.4 Quiché earthquake is the deepest recorded major ($M_w > 6$) earthquake to have occurred in the Cocos slab beneath Central America, at a depth of $\sim$ 255 km. Here, we refine the source parameters of both the Quiché earthquake, and the only other event at comparable depths (the 1997 M_w 5.5 Jutiapa earthquake), confirming both their exceptional depth within the downgoing slab, and their down-dip extensional mechanism. That the Cocos slab remains capable of hosting major intraslab earthquakes, with mechanisms consistent with down-dip extension, near, or at, the tip of the contiguous slab, suggests that the slab itself is weak, such that the minimal stresses derived from supporting the negative buoyancy of the short section of slab down-dip from this earthquake are still sufficient to lead to brittle failure of the slab.

Resumen El terremoto de Quiché de magnitud M_w 6.4 en 2023 es el terremoto de mayor magnitud ($M_w > 6$) registrado en la zona más profunda de la placa de Cocos bajo América Central, a una profundidad de $\sim$ 255 km. Aquí, refinamos los parámetros fuente tanto para el terremoto de Quiché como para el único otro evento a profundidades comparables (el terremoto de Jutiapa de magnitud M_w 5.5 en 1997), confirmando tanto su profundidad excepcional dentro de la placa descendente, como su consistente mecanismo extensional hacia abajo. Que la placa de Cocos siga siendo capaz de experimentar terremotos intra-slab de gran magnitud, con consistentes mecanismos de extensión hacia abajo, cerca o en el borde con la placa contigua, sugiere que la placa misma es débil, a tal punto que las tensiones mínimas derivadas de este terremoto, asociadas a la flotabilidad negativa de la pequeña sección de la placa descendente, siguen siendo suficientes para producir el fracturamiento frágil de la placa.

Production Editor: Gareth Funning
Handling Editor: Marino Protti
Copy & Layout Editor: Théa Ragon

Received: January 24, 2024
Accepted: March 22, 2024
Published: May 28, 2024

1 Introduction

The oceanic Cocos plate subducts beneath Central America along the Middle America Trench, giving rise to both widespread seismicity on the subduction megathrust and to prolific (although unevenly distributed) seismicity within the Cocos slab as it descends into the upper mantle. Although contributing only a small proportion of the overall moment release associated with the Central American subduction zone, intraslab events can, on occasion, be both large and damaging. In the case of Central America, these intraslab events include the damaging M_w7.7 2001 El Salvador earthquake (Vallée et al., 2003), the M_w7.4 1999 Oaxaca/Tehuacán earthquake (Singh et al., 2000), and the 2017 M_w8.2 Tehuantepec and M_w7.1 Puebla earthquakes (Melgar et al., 2018a,b).

In its northern sections, the Central American slab is dominated by the flat slab region under southern Mexico (e.g., Kim et al., 2010; Manea et al., 2017). East of $\sim$ 97° W, the slab transitions via a region of probable slab tearing (e.g., Rogers et al., 2002; Manea et al., 2013) to a more classical slab geometry, dipping gently down into the upper mantle (e.g., Syracuse et al., 2008; Manea et al., 2013). East of the flat slab region, the slab shows a fairly consistent geometry, characterised by its dip gradually increasing from $< 20°$ to $> 60°$ at fairly consistent slab curvatures (Hayes et al., 2018). Current slab models suggest the contiguous downdip slab extends to depths of $\sim$ 250-300 km — below this depth, the nature of the slab becomes unclear, with different data suggesting either a gap between the shallow slab and a detached slab in the mid mantle (Rogers et al., 2002) or a fragmentary, perforated, slab subject to through-going mantle flow (Zhu et al., 2020; Xue et al., 2023).

The causative rheological mechanism allowing brittle failure in such intraslab earthquakes to occur remains uncertain, with both dehydration embrittlement and shear-heating driven thermal instability remaining as viable candidates (e.g., Hosseinzadehsabeti et al., 2021; Wimpenny et al., 2023; Prakash et al., 2023). However, no matter what the rheological control allowing seismogenic failure is, the consistency and regional coherency of deformation illuminated by intraslab seismicity requires that their spatial occurrence is controlled by the intraslab stress state – well established to be a function of the interplay between stresses related

*Corresponding author: t.j.craig@leeds.ac.uk

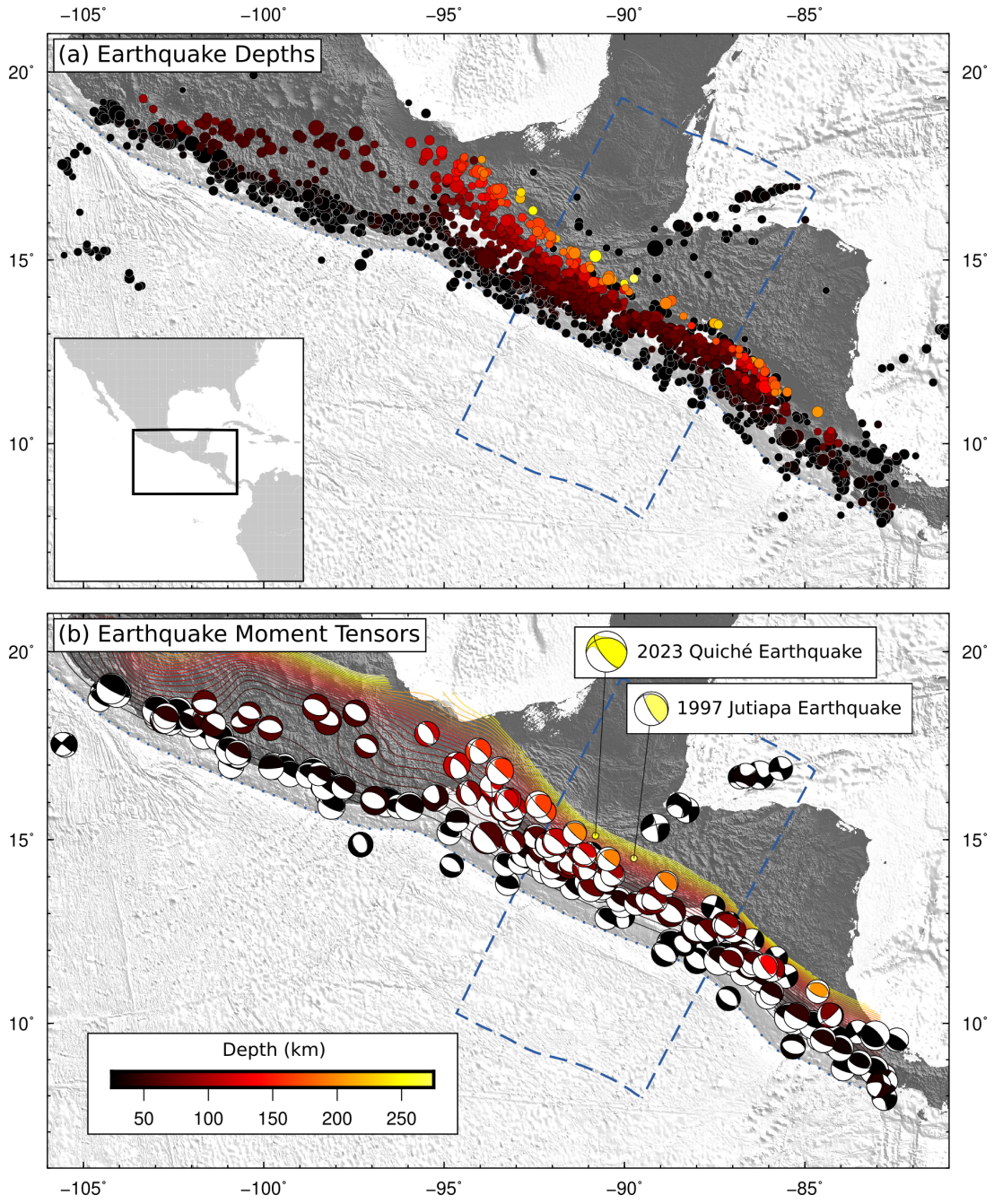

Figure 1 Earthquakes along the Central American Subduction Zone. (a) Earthquake depths. Inset panel shows a regional location map; (b) Earthquake moment tensors, from the gCMT catalogue. Compressional quadrants are shaded by earthquake depth. Inset boxes highlight the 2023 Quiché and 1997 Jutiapa earthquakes, and use our moment tensors and locations. Contours show the Slab2 model (Hayes et al., 2018). Dashed blue box shows the region used in plotting the cross sections shown in Figure 5.

to the negative buoyancy of the slab (slab pull), tractions on the edge of the slab from its interaction with the surrounding mantle, stresses relating to the bending and unbending of the slab, and stresses arising from the evolving thermochemical state of the slab (e.g., thermal expansion, volumetric changes resulting from mineralogical phase transitions) (e.g., Manea et al., 2006; Bailey et al., 2012). The dominant two are believed to be slab pull, which plays a role in driving global plate tectonics, and the bending stresses. Which of these dominates the overall stress state of the slab likely varies between different geodynamic settings (Sandiford et al., 2020; Craig et al., 2022; Sippl et al., 2022).

This study focuses on the M_w 6.4 2023 Quiché earthquake (Figure 1), which occurred beneath the central Guatemalan cordillera on the 17^{th} May 2023, at 23:02:00 (UTC). Preliminary locations placed this earthquake at depths of ~ 255 km (as reported by the NEIC; please see Table 1), at the leading edge of the contiguous section of the subducting Cocos slab beneath Central America. The depth and location of this earthquake make it stand out against the backdrop of other seismicity associated with the Central American slab – both as a comparatively large-magnitude event for the Central American slab, but also as one at substantially greater depths than generally recorded for earthquakes in the slab beneath

Origin time (UTC)		Method	Lat (°)	Long (°)	Depth (km)	M_w	M_{rr}	M_{tt}	M_{pp}	M_{rt}	M_{rp}	M_{tp}	γ
2023/05/17	23:02:00.5	NEIC	15.181	-90.815	253.5	6.4	-	-	-	-	-	-	-
	23:02:03.2	gCMT	15.17	-90.99	253.0	6.4	0.305	-0.334	0.030	0.326	-0.525	0.124	84%
	23:02:05.6	This Study	14.82‡	-91.12‡	256.0	6.4	0.449	-0.375	-0.074	0.222	-0.428	0.306	94%
1997/05/15	04:39:21.5	NEIC	14.460	-89.775	274.2	4.9†	-	-	-	-	-	-	-
	04:39:23.3	ISC-EHB	14.490	-89.741	279.4	4.9†	-	-	-	-	-	-	-
	04:39:26.3	gCMT	14.53	-89.85	272.9	5.5	0.170	-0.072	-0.073	0.315	-0.616	0.043	92%
	04:39:25.6	This Study	14.12‡	-89.82‡	270.0	5.5	0.328	-0.213	-0.115	0.276	-0.568	0.136	85%

Table 1 Earthquake source parameters from different seismic catalogues. Note that at the time of writing no solution is yet available for the 2023 Quiché earthquake from the ISC. Magnitudes denoted † are instead m_b rather than M_w. Locations marked with ‡ are unreliable.

Central America. Along with the 2023 Quiché earthquake, we also revisit a M_w 5.5 earthquake from 15^{th} May 1997, which occurred under Jutiapa in southeastern Guatemala, ~150 km ESE along the strike of the subduction zone from the Quiché earthquake, but at a similar depth – also at the leading edge of the contiguous slab. Together, these two earthquakes represent the two deepest larger-magnitude events, and define the tip of the seismogenic slab.

Here, we present a refinement of the seismologically-determined source parameters of these two earthquakes, consider their geodynamic context within the Cocos plate, and the implications of such deep intraslab earthquakes for the force-balance of the subducting plate.

2 Earthquake source parameter determination

We refine initial estimates of the source parameters of the Quiché and Jutiapa earthquakes using global seismic data. We use the Grond software of Heimann et al. (2018) to invert seismological waveform data for the earthquake location (latitude, longitude, depth), source duration, magnitude, and six components of the moment tensor. We draw on both vertical and horizontal component data recorded at teleseismic distances (30° – 90°) from the earthquake epicentre. Horizontal components are rotated into earthquake-relative radial and transverse components. Station response functions are removed from all seismograms, and data are filtered to frequencies of 0.025 – 0.25 Hz using a four-pole Butterworth bandpass.

We use vertical component data to invert for the direct *P*-wave and its associated depth phases, and both radial and transverse data to invert for the *S*-wave and its associated depth phases. Misfits from radial and transverse component waveforms are downweighted during inversion by a factor of two, to reduce over-fitting of the usually higher-amplitude *S*-wave and its depth phases. Inversion windows are taken from 20 seconds before the predicted onset of each direct phase, to 120 after – a time range estimated to encompass the direct arrival and principal depths phases (*pP, sP, pS, sS*), based on the initial catalogue depth, and verified visually. Whilst the majority of similar studies use only vertical and transverse component data, we find here that the additional use of radial component data, in this case, makes a minor improvement in the resolution of the source mechanism, due to the inclusion of the *pS* depth phase, particularly for the Quiché event.

We invert for the six components of the moment tensor (constrained to be purely deviatoric with no isotropic component), along with three location parameters, moment, and source duration. Synthetic and observed waveforms are realigned during each iteration using on a time shift which maximises the cross correlation value between the observed and synthetic traces at each station and for each component independently.

Information about the velocity structure of the overriding Central American plate is limited, in comparison to other subduction zones, due to the relative sparsity of near-field instrument deployments. As a result, we use a velocity structure based on the global ak135 velocity model (Kennett et al., 1995). Given the inclusion of a waveform-realignment step in the inversion approach, our modelling is most sensitive to the velocity structure at depths between the earthquake source and the free surface. This being the case, our results are not particularly impacted by the lack of a fast, cold mid-mantle slab in ak135, and this does not have a significant impact on the determination of either source depth or source mechanism. However, teleseismic source inversions, especially in cases where station-specific temporal realignment is included, are typically insensitive to small changes in the lateral location of the earthquake. As such, although we do allow our inversion to re-determine source latitude and longitude (see Table 1), we note that these are poorly constrained, with substantial variability in the range of acceptable solutions, and therefore we consider these parameters to be unreliable.

Figures 2 and 3 show inversion results for the Quiché and Jutiapa earthquakes respectively, showing example radial, transverse and vertical component waveforms, the resultant probabilistic moment tensor, and parameter histograms for depth, strike, dip, rake, and the degree to which the mechanism contains any non-double couple (nDC) component. In this case, we assume that a well-constrained mechanism would be a pure double couple, and that any nDC component would reflect the mapping of noise into the solution. For both events, the nDC moment required is only a small fraction of the overall moment release required, indicating that

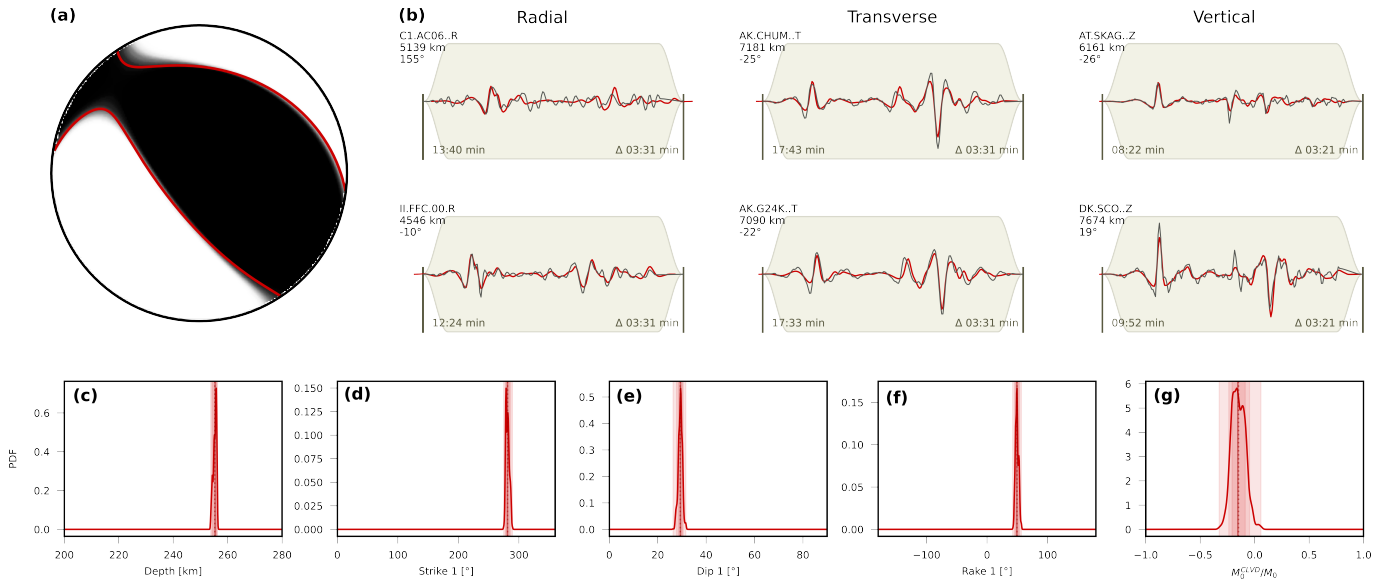

Figure 2 Earthquake source determination results for the 2023 Quiché earthquake. (a) Probabilistic moment tensor. Red lines show the minimum misfit moment tensor. (b) Observed waveforms (black) and calculated synthetics (red) for the minimum misfit solution. Shown are 6 examples traces, two each for radial, transverse and vertical components. Note that the instruments shown for each component varies. Annotations give the network and station name, epicentral distance, azimuth, trace start time, and inversion window length. (c) – (g) show probability density functions for depth, strike, dip, rake, and the ratio of the moment proportions allocated as a compensated linear vector dipole (CLVD) to the overall moment.

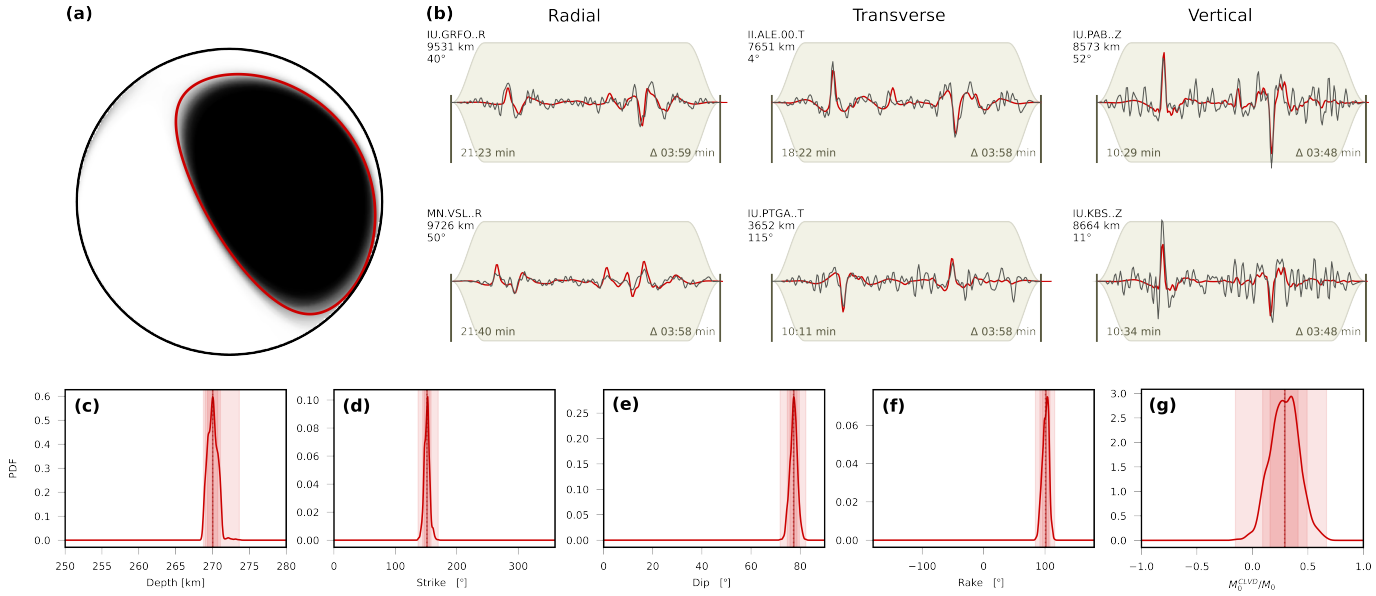

Figure 3 Earthquake source determination results for the 19997 Jutiapa earthquake. Panels are as shown in Figure 2.

our solutions are reasonably well constrained, and free from significant noise influence – a conclusion visually supported by inspection of the waveforms in Figures 2 and 3, which shows clear, relatively noise-free phase arrivals.

As the waveform fits in Figures 2 and 3 show, we are able to fit both the timing and amplitude of multiple phases across the waveform sections used. Both of our two earthquakes yield well-constrained depths, with Jutiapa being slightly deeper (270 km) than the Quiché event (256 km). These events are verified to be the deepest significant earthquakes within the Cocos plate yet recorded using global seismic data.

Whilst the two earthquakes differ slightly in their mechanism, due to the different signs of their small nDC components, the double couple component of their respective mechanisms is overall similar, representing almost pure dip-slip faulting, striking marginally obliquely to the strike direction of the slab, with a steeply-dipping southeast striking nodal plane, and a shallowly-dipping northwest striking nodal plane. Mechanism orientation parameters in all cases are extremely well constrained, and are consistent with the orientation of faulting within the Cocos slab in other earthquakes deeper than $\sim$ 150 km.

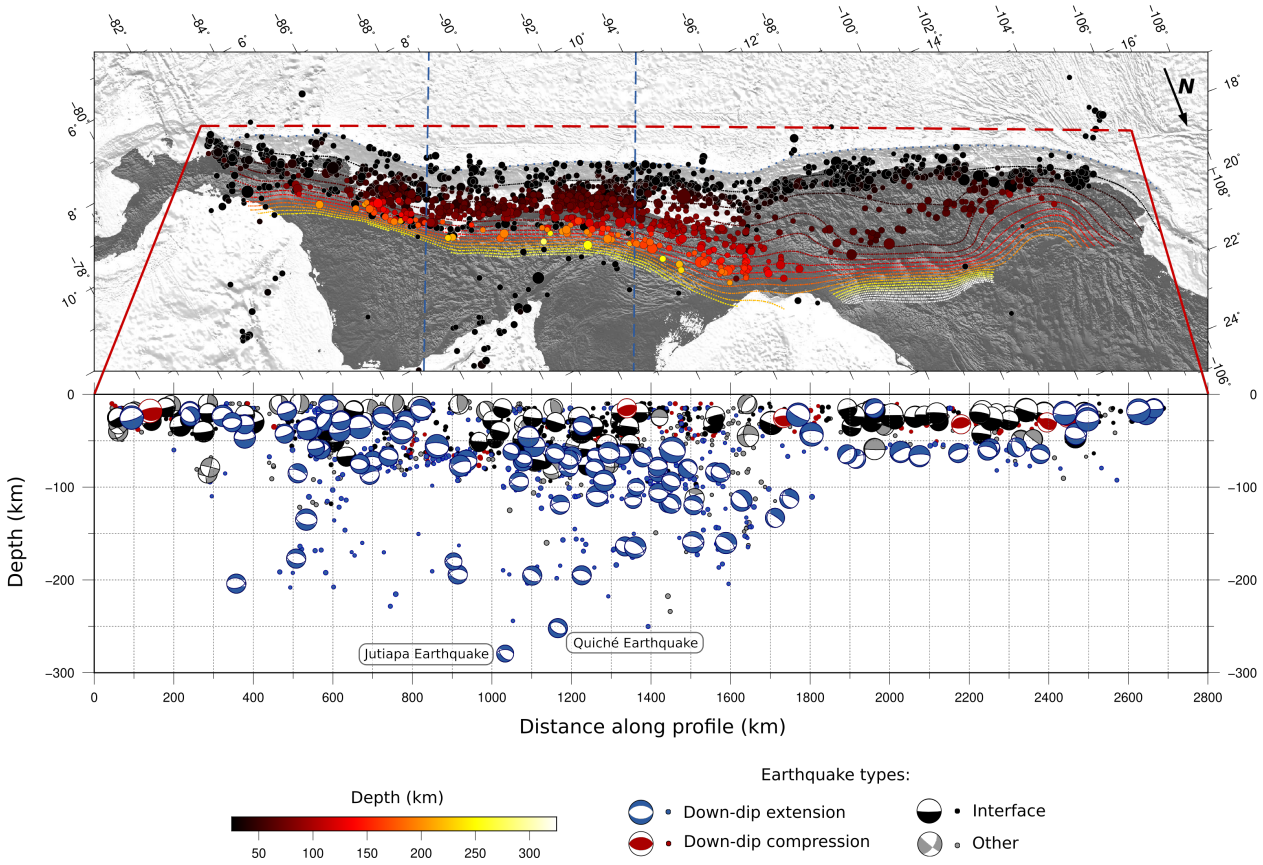

Figure 4 Reprojected earthquake moment tensors in the Central American Subduction Zone. Upper panel shows earthquake locations, coloured by depth. Contours show the slab model of (Hayes et al., 2018). Blue lines show the limits of the cross section shown in Figure 5, red line shows the projection line for the lower panel. Lower panel shows earthquake locations as a function of depth and distance along the projection line shown in the upper panel. Moment tensors (for earthquakes with $M_w \geq 6.0$ are rotated in three dimensions to be in a slab-relative reference frame appropriate for the location of the earthquake and its local slab geometry. The moment tensor for the 1997 Jutiapa earthquake is plotted despite having an M_w of 5.5.

3 Seismicity with the Central American Slab

In Figure 4, we show subduction-related seismicity along the Central American subduction zone, reprojected into a slab-relative reference frame such that the focal mechanisms shown are relative to the local slab surface from the Slab2 model of Hayes et al. (2018). Figure 5 shows a cross section through the slab beneath Guatemala, including a reprojection into slab-relative coordinates in Figure 5b.

Although in map view (e.g. Figure 1), many of the deeper earthquakes within the Cocos slab appear to be thrust-faulting earthquakes, when considered in a slab-relative reference frame, earthquakes within the slab instead almost entirely reflect down-dip extension within the slab. As Figure 5 demonstrates, intraplate faulting is dominated by downdip extension almost perfectly aligned to the direction of the slab dip. The slight mis-alignment between the strike of active intraslab faults and the slab strike (visible on Figure 4 and Figure 5a) probably reflects the slight misalignment between the trench orientation and the relict fabric of the incoming Cocos plate, reactivated in the outer rise (e.g., Masson, 1991; Ranero et al., 2005), and which likely remains active in the intraslab environment (Boneh et al., 2019).

The majority of slabs globally show a diversity of intraslab focal mechanisms, with a mix of both downdip compression and downdip extension, typically separated into discrete planes (double seismic zones) within the slab (Isacks and Molnar, 1969; Sandiford et al., 2019, 2020; Craig et al., 2022; Sippl et al., 2022). However, as we see from Figures 4 and 5, the Cocos slab stands out against this trend – almost all of the intraslab seismicity below ~75 km depth reflects down-dip extensional stresses. As Figure 5a shows these earthquakes show a remarkable degree of consistency in their slab relative mechanism orientations – a result of a relatively simple intraslab stress field, presumably dominated by slab pull, and with minimal impact from bending-related stresses after the initial phase of post-subduction unbending, reflected in the simple slab geometry seen beneath Guatemala on Figure 5c.

However, of particular note here is that both the Quiché and Jutiapa earthquakes occur at the very leading edge of the contiguous Cocos slab, in a region where the slab is subject to neither substantial bending-related stresses, nor to major buoyancy forces relating to the presence of a substantial high-density down-dip slab. Despite this, both earthquakes show complete consis-

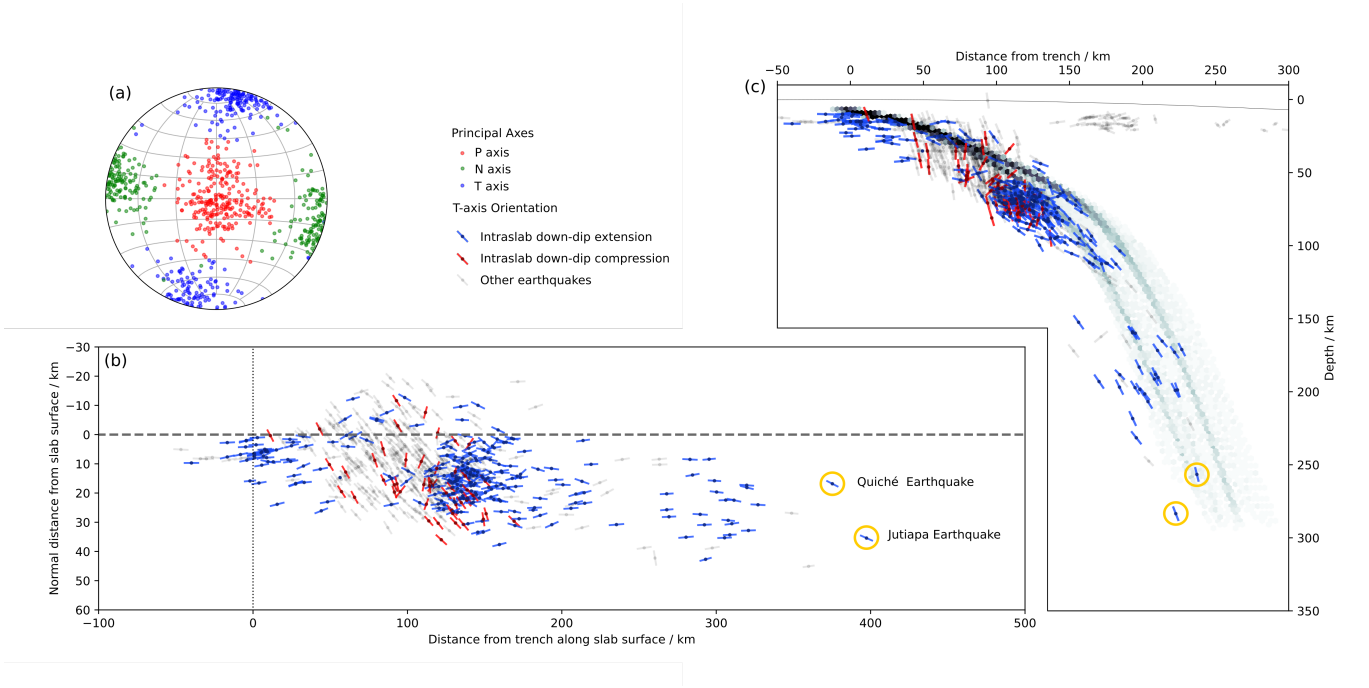

Figure 5 (a) Slab-relative orientations of the principal axes for the population of earthquakes consistent with down-dip extension. (b) Trench-perpendicular cross section for the region between the blue lines on Figure 1. Earthquakes locations are given by circular points, underlain by bars indicating the inclination of the T axis. Bars are coloured blue for those events consistent with down-dip extension, red for those consistent with down-dip compression, and grey for all other earthquakes. Locations are reprojected to show trench-perpendicular distance relative to the local trench. Background shows the variation in slab geometries across the region. Yellow circles highlight the 2023 Quiché and 1997 Jutiapa earthquakes. (c) Cross section showing earthquake locations and moment-tensor orientations in a reference frame relative to the local slab surface.

tency in orientation with the rest of the intraslab deformation field. The Quiché earthquake also stands out for its magnitude – although not, by a long way, the largest intraslab event recorded within the Cocos plate, a M_w 6.4 would be expected to require a fault area on the order of $\sim$ 100 km^2, requiring either a high-aspect-ratio rupture, or a substantial seismogenic cross section for the slab at this depth.

4 Dynamics of the Central American Slab

Simple numerical calculations in the wake of the development of early slab models explored the evolution of the intraslab stress state as a function of the slab length (e.g., Vassilou et al., 1984; Vassilou and Hager, 1988), assuming that the slab behaves as a Newtonian fluid coupled to a less viscous surrounding mantle and deforming under its own weight, descending into a layered mantle structure. Such models neglect any bending-related stresses, and any stress variations resulting from the internal rheological evolution of the slab, and therefore simply provide estimates of the intraslab stress field driven by slab pull and the interaction of the slab with the surrounding mantle. We do not attempt to reproduce the calculations of Vassilou and Hager (1988) here, but summarise their findings in Figure 6. The negative buoyancy of the slab in each case puts the shallow part of the slab into down-dip extension, whilst for slabs extending towards the mantle transition zone, where there is a significant viscosity contrast, there is a switch into down-dip compression in the deeper parts of the slab, which propagates back to increasingly shallower depths for slab that reach deeper into the mantle. The dashed line on Figure 6 shows the impact of having an inclined slab, rather than a vertical one – essentially, this serves to reduce the magnitude of the stresses involved, and produces a rotation in the local stress tensor, but has little impact on the 'polarity' of the stress field, with shallow depths still being dominated by down-dip extensional stresses. The Cocos slab under Guatemala would most closely resemble the '270' km slab model shown in Figure 6. Of note here is that the predicted stresses near the slab tip are very low, due to the small length of negatively buoyant slab extending to greater depths. We also note that for slabs only reaching to $\sim$300 km, the tip of the slab is not placed into down-dip compression, as it remains too distant from the mantle transition zone.

At this time, we are not aware of any concrete evidence that the Cocos slab persists significantly below $\sim$300 km as a contiguous structure (i.e., one which can act as a stress guide) – whilst there is clearly slab-derived material deeper into the mantle (e.g., Rogers et al., 2002), how this connects to the shallow slab is unclear, with no clear evidence for a down-dip continuous slab. In models which do image the continuation of slab-derived material below 300 km (e.g., Zhu et al., 2020; Xue et al., 2023), the weak velocity anomaly, combined with the orientation of mantle fabrics, is interpreted to show a fragmentary slab subject to through-going mantle flow. We do, however, note that further work on

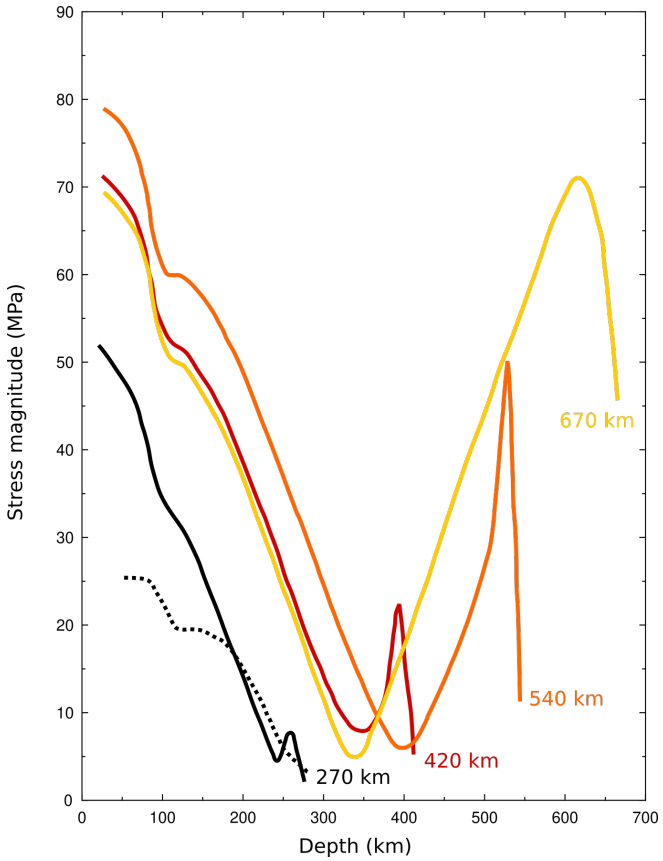

Figure 6 Stress as a function of depth for variable length slabs, descending under their own weight into a viscous mantle. All slabs are assumed to dip vertically, except for the dashed line, which dips at 45°. The in-plane stress field within the slab is in down-dip extension at shallow depths, with the increase beyond ∼350 km reflecting a switch to down-dip compression due to interaction of the slab tip with the viscosity increase at the transition zone (670 km). After Vassilou and Hager (1988).

imaging the Cocos slab beneath Central America may change this picture, and our subsequent interpretation.

Under the assumption that the Cocos slab does not persist below ∼300 km in a manner capable of sustaining significant stresses, it is notable that, even at the very tip of the contiguous Cocos slab, the slab remains capable of producing earthquakes such as those beneath Quiché and Jutiapa. The slab-pull derived intraslab stress field should, at the tip of the slab, become small, yet the consistency between the orientation of these earthquakes at 250–270 km depths, and those between 120–250 km, suggests that a similar interplay of stress field and relict structure continues to control the orientation of faulting throughout the slab, potentially modulated by the availability of a brittle rheology dependent on localised hydration along pre-existing structure. Two implications arise from this observation:

- that, in the absence of bending-related stresses, the buoyancy-related stresses (i.e., slab pull) continue to dominate the intraslab stress field, even in environments where these stresses must be small. Other sources of stress (e.g., those arising from the thermo-chemical evolution of the slab), must therefore be insignificant.

- that the slab itself must be rheologically quite weak, such that even the reduced buoyancy-related stresses present near the slab tip remain capable to activating, in the case of the Quiché earthquake, a substantial seismogenic cross section of the slab.

5 The mechanics of intermediate depth earthquakes

In keeping with other intermediate depth earthquakes (e.g., Ye et al., 2020; Wimpenny et al., 2023), both the Quiché and Jutiapa earthquakes had low-productivity aftershock sequences. Despite its own considerable magnitude (M_w 6.4), the Quiché earthquake was reported by the NEIC to be followed by only two other earthquakes within 100 km of the earthquake epicentre in the following 6 months, both considerably smaller (m_b 4.6 and 4.3) and considerably shallower ($<$ 200 km). Following the 1997 Jutiapa earthquake, the NEIC reported only one aftershock near the intermediate-depth source region, with m_b 4.9. The lack of a substantial aftershock population also inhibits the inference of earthquake rupture dimensions and causative fault plane based on aftershock distribution and extent, although we note the potential for local seismic data to clarify this (e.g., Yani-Quiyuch et al., 2023).

That the deviatoric stress derived from the negative buoyancy of the short section of the contiguous slab down-dip from these earthquakes was still capable of producing major seismogenic failure of the slab suggests that the yielding stress of the slab at such depth was also low – a condition more easily reconcilable with the rheological control on intraslab seismicity being related to either dehydration embrittlement or dehydration stress transfer, either of which would greatly reduce the effective yield stress, rather than a shear-heating model, which would still require high stresses to initiate the initial shear instability.

6 Conclusions

The Quiché and Jutiapa earthquakes represent down-dip extensional failure near the tip of the subducting Cocos slab beneath Guatemala. The coherence of the moment tensors of these earthquakes with those updip suggests that the intraslab stress field at such depths remains dominated by the negative buoyancy of the slab (slab pull). That the slab at such depths remains capable of major seismogenic failure in down-dip extension, despite the limited section of contiguous slab extending beyond the depth of these earthquakes, suggests that the slab itself is relatively weak, in order to allow failure under only low-magnitude slab pull-derived stresses. The sensitivity of the slab to relatively small deviatoric stresses (compared to lithostatic stresses), is consistent with a fluid-related rheological control on intraslab seismicity.

Acknowledgements

The authors were supported in this work by the Royal Society under URF\R1\180088 and URF\R\231019. TJC was also supported through COMET, the UK Natural Environment Research Council's Centre for the Observation and Modelling of Earthquakes, Volcanoes, and Tectonics. The numerical modelling component of this work was undertaken on ARC4, part of the High Performance Computing facilities at the University of Leeds, UK.

Data and code availability

We are extremely grateful to all those involved in the deployment and maintenance of the seismological networks whose data we draw on. We draw on seismological catalogues from the gCMT project (https://www.globalcmt.org; last accessed 22/1/2023), and from the International Seismological Centre (http://www.isc.ac.uk; last accessed 22/1/2023). This work principally used code provided as part of the Generic Mapping Tools (Wessel et al., 2013), and via the Pyrocko toolbox (https://pyrocko.org, Heimann et al., 2017). Waveform inversions were carried out using the Grond software of Heimann et al. (2018).

Competing interests

The authors declare no known competing interests.

References

Bailey, I. W., Alpert, L. A., Becker, T. W., and Miller, M. S. Co-seismic deformation of deep slabs based on summed CMT data. *Journal of Geophysical Reearch*, 117, 2012. doi: 10.1029/2011JB008943.

Boneh, Y., Schottenfels, E., Kwong, K., van Zelst, I., Tong, X., Eimer, M., Miller, M., Moresi, L., Warren, J., Wiens, D., nd J. Naliboff, M. B., and Zhan, Z. Intermediate-depth earthquakes controlled by incoming plate hydration along bending-related faults. *Geophysical Research Letters*, 46:3688–3697, 2019. doi: 10.1029/2018GL081585.

Craig, T., Methley, P., and Sandiford, D. Imbalanced moment release within subducting places during initial bending and unbending. *Journal of Geophysical Research*, 127, 2022. doi: 10.1029/2021JB023658.

Hayes, G., Moore, G., Portner, D., Hearne, M., Flamme, H., Furtney, M., and Smocyzk, G. Slab2, a comprehensive subduction zone geometry. *Science*, 2018. doi: 10.1126/science.aat4723.

Heimann, S., Kriegerowski, M., Isken, M., Cesca, S., Daout, S., Grigoli, F., Juretzek, C., Megies, T., Nooshiri, N., Steinberg, A., Sudhaus, H., Vasyura-Bathke, H., Willey, T., and Dahm, T. Pyrocko - An open-source seismology toolbox and library. *GFZ Data Services*, 2017. doi: 10.5880/GFZ.2.1.2017.001.

Heimann, S., Isken, M., Kuhn, D., Sudhaus, H., Steinberg, A., Vasyura-Bathke, H., Daout, S., Cesca, S., and Dahm, T. Grond - A probabilistic earthquake source inversion framework. *GFZ Data Services*, 2018. doi: 10.5880/GFZ.2.1.2018.003.

Hosseinzadehsabeti, E., Ferre, E., Persaud, P., Fabbri, O., and Geissman, J. The rupture mechanisms of intraslab earthquakes: a multiscale review and re-evaluation. *Earth Science Reviews*, 221, 2021. doi: 10.1016/j.earscirev.2021.103782.

Isacks, B. and Molnar, P. Mantle earthquake mechanisms and the sinking of the lithosphere. *Nature*, 223:1121–1124, 1969.

Kennett, B. L. N., Engdahl, E. R., and Buland, R. Constraints on seismic velocities in the Earth from travel times. *Geophysical Journal International*, 122:108–124, 1995.

Kim, Y., Clayton, R., and Jackson, J. Geometry and seismic properties of the subducting Cocos plate in central Mexico. *Journal of Geophysical Research*, 115, 2010. doi: 10.1029/2009JB006942.

Manea, V., Manea, M., Kostoglodov, V., and Sewell, G. Intraslab seismicity and thermal stress in the subducted Cocos plate beneath central Mexico. *Tectonophysics*, 420, 2006. doi: 10.1016/j.tecto.2006.03.029.

Manea, V., Manea, M., and Ferrari, L. A geodynamical perspective on the subduction of Cocos and Rivera plates beneath Mexico and Central America. *Tectonophysics*, 609:56–81, 2013. doi: 10.1016/j.tecto.2012.12.039.

Manea, V., Manea, M., Ferrari, L., Orozco-Esquivel, T., Valenzuela, R., Husker, A., and Kostoglodov, V. A review of the geodynamic evolution of flat slab subduction in Mexico, Peru and Chile. *Tectonophysics*, 695:27–52, 2017. doi: 10.1016/j.tecto.2016.11.037.

Masson, D. G. Fault Patterns at Outer Trench Walls. *Marine Geophysical Researches*, 1991:209–225, 1991.

Melgar, D., Pérez-Campos, X., Ramirez-Guzman, L., Spica, Z., Espíndola, V., Hammond, W., and Cabral-Cano, E. Bend Faulting at the Edge of a Flat Slab: The 2017 M_W 7.1 Puebla-Morelos, Mexico, Earthquake. *Geophysical Research Letters*, 45:2633–2641, 2018a. doi: 10.1002/2017GL076895.

Melgar, D., Ruiz-Angula, A., Garcia, E., Manea, M., Manea, V., Xu, X., Ramirez-Herrera, M., Zavala-Hidalgo, J., Geng, J., Corona, N., Pérez-Campos, X., Cabral-Cano, E., and Ramirez-Guzmán, L. Deep embrittlement and complete rupture of the lithosphere during he M_w 8.2 Tehuantepec earthquake. *Nature Geoscience*, pages 955–960, 2018b. doi: 10.1038/s41561-018-0229y.

Prakash, A., Holyoke III, C., Kelemen, P., Kirby, S., Kronenberg, A., and Lamb, W. Carbonates and intermediate-depth seismicity: Stable and unstable shear in altered subducting plates and overlying mantle. *Proceedings of the National Academy of Sciences*, 120, 2023. doi: 10.1073/pnas.2219076120.

Ranero, C. R., Villaseñor, A., Morgan, J. P., and Weinrebe, W. Relationship between bend-faulting at trenches and intermediate-depth seismicity. *Geochemistry, Geophysics, Geosystems*, 6, 2005. doi: 10.1029/2005GC0009972.

Rogers, R., Kárason, H., and van der Hilst, R. Epeirogenic uplift above a detached slab in northern Central America. *Geology*, 30:1031–1034, 2002. doi: 10.1130/0091-7613(2002)030.

Sandiford, D., Moresi, L., Sandiford, M., and Yang, T. Geometric controls on flat slab seismicity. *Earth and Planetary Science Letters*, 527, 2019. doi: 10.1016/j.epsl.2019.115787.

Sandiford, D., Moresi, L., Sandiford, M., Farrington, R., and Yang, T. The Fingerprints of Flexure in Slab Seismicity. *Tectonics*, 39, 2020. doi: 10.1029/2019TC005894.

Singh, S., Ordaz, M., Alcántara, L., Shapiro, N., Kostoglodov, V., Pacheco, J., Alcocer, S., Gutiérrez, C., Quass, R., Mikumo, T., and Ovando, E. The Oaxaca Earthquake of 30 September 1999 (Mw = 7.5): A Normal-faulting Event in the Subducted Cocos Plate. *Seismological Research Letters*, 71:67–78, 2000. doi: 10.1785/gssrl.71.1.67.

Sippl, C., Dielforder, A., John, T., and Schmalholz, S. Global Constraints on Intermediate-Depth Intraslab Stresses From Slab Geometries and Mechanisms of Double Seismic Zone Earthquakes. *Geochemistry Geophyics Geosystems*, 23, 2022. doi: 10.1029/2022GC010498.

Syracuse, E., Abers, G., Fischer, K., MacKenzie, L., Rychert, C., Protti, M., González, V., and Strauch, W. Seismic tomography and earthquake locations int he Nicaragua and Costa Rican upper mantle. *Geochemistry Geophysics Geosystems*, 9, 2008. doi: 10.1029/2008GC001963.

Vallée, M., Bouchon, M., and Schwartz, S. Y. The 13 January 2001 El Salvador earthquake: A multidata analysis. *Journal of Geophysical Research*, 108, 2003. doi: 10.1029/2002JB001922.

Vassilou, M. and Hager, B. Subduction Zone Earthquakes and Stress in Slabs. *Pure and Applied Geopysics*, 128:547–624, 1988. doi: 10.1007/BF00874550.

Vassilou, M., Hager, B., and Raefsky, A. the distribution of earthquakes with depth and stress in subducting slabs. *Journal of Geodynamics*, 1:11–28, 1984. doi: 10.1016/0264-3707(84)90004-8.

Wessel, P., Smith, W., Scharroo, R., Luis, J., and Wobbe, F. Generic Mapping Tools: Improved version released. *EOS Transactions*, 94:409–410, 2013.

Wimpenny, S., Craig, T., and Marcou, S. Re-Examining Temporal Variations in Intermediate-Depth Seismicity. *Journal of Geophysical Research*, 128, 2023. doi: 10.1029/2022JB026269.

Xue, T., Peng, D., Liu, K., Obrist-Farner, J., Locmelis, M., Gao, S., and Liu, L. Ongoing fragmentation of the usubducting Cocos slab, Central America. *Geology*, 51, 2023. doi: 10.1130/G51403.1.

Yani-Quiyuch, R., Asturias, L., and Castro, D. The rupture plane of the 16 February 2022 M_w 6.2 Guatemala, intermediate depth earthquake. *Seismica*, 2.2, 2023. doi: 10.26443/seismica.v2i2.691.

Ye, L., Lay, T., and Kanamori, H. Anomalously low aftershock productivity of the 2019 Mw 8.0 energetic intermediate-depth faulting beneath Peru. *Earth and Planetary Science Letters*, 549, 2020. doi: 10.1016/j.epsl.2020.116528.

Zhu, H., Stern, R., and Yang, J. Seismic evidence for subduction-induced mantle flows underneath Middle America. *Nature Communications*, 11, 2020. doi: 10.1038/s41467-020-15492-6.